

Carbon Dioxide Reduction by Pincer Rhodium η^2 -Dihydrogen Complexes: Hydrogen-Binding Modes and Mechanistic Studies by Density Functional Theory Calculations

Kuo-Wei Huang,^{*,†} Joseph H. Han,[‡] Charles B. Musgrave,[‡] and Etsuko Fujita^{*,†}

Chemistry Department, Brookhaven National Laboratory, Upton, New York 11973, and Department of Chemical Engineering, Stanford University, Stanford, California 94305

Received September 1, 2006

Density functional theory (DFT) calculations using the KMLYP method on a series of pincer PCP–rhodium dihydrogen complexes have been employed to model and examine the proposed mechanisms for the pincer PCP–rhodium complexes mediated hydrogenation of carbon dioxide (CO₂). The relative energies of dihydrogen rotamers and dihydride isomers were evaluated together with T_1 values to determine the molecular structures of these complexes. We have investigated possible pathways for the CO₂ reduction processes involving the formation of rhodium dihydride species. Although the dihydrogen complexes are more stable than the corresponding dihydride isomers, the reduction of CO₂ has to proceed through the dihydride structures.

Introduction

Transition metal-catalyzed homogeneous hydrogenation of carbon dioxide (CO₂) has attracted much interest and continues to receive significant attention because of its relevance in carbon management research and its potential to serve as a source for the C1 feedstock from the abundant gas CO₂.^{1–4} A number of effective rhodium and ruthenium complexes have been reported to catalyze the hydrogenation of CO₂ in a variety of solvents.^{5–17}

Kinetic studies of these systems along with theoretical calculations have greatly improved the mechanistic understanding of the important steps in the catalytic cycles.^{18–25} It is well accepted that the first critical step of the reduction is the insertion of a CO₂ molecule into a metal–hydride bond. On the other hand, mechanistic studies on the hydrogenation of carbon dioxide mediated by complexes lacking a metal–hydride bond have not been documented.

In 1988, Kaska and co-workers reported a CO₂ hydrogenation reaction by a pincer rhodium dihydrogen complex that was referred to as “{2,6-bis[(di-*tert*-butylphosphino)methyl]phenyl}dihydridorhodium(III)” (hereafter denoted as complex **1**).²⁶ This complex was synthesized by reduction of the {2,6-bis[(di-*tert*-butylphosphino)methyl]phenyl}hydridorhodium chloride precursor²⁷ with potassium hydride under 1 atm of dihydrogen gas.²⁸ While these authors did not comment on whether this “dihydrido” complex was a classical or nonclassical dihydrogen complex, they showed that it was capable of reducing CO₂. Interestingly, the first stable intermediate observed was a hydridorhodium hydroxide complex (**3**), presumably through the hydridorhodium formate intermediate **2**. Complex **3** then

* Authors for correspondence. E-mail: hkw@bnl.gov (K.-W.H.); fujita@bnl.gov (E.F.).

[†] Brookhaven National Laboratory.

[‡] Stanford University.

(1) Leitner, W. *Angew. Chem., Int. Ed. Engl.* **1995**, *34*, 2207–2221.

(2) Jessop, P. G.; Ikariya, T.; Noyori, R. *Chem. Rev.* **1995**, *95*, 259–272.

(3) Jessop, P. G.; Joo, F.; Tai, C. C. *Coord. Chem. Rev.* **2004**, *248*, 425–2442.

(4) Arakawa, H.; Aresta, M.; Armor, J. N.; Barteau, M. A.; Beckman, E. J.; Bell, A. T.; Bercaw, J. E.; Creutz, C.; Dinjus, E.; Dixon, D. A.; Domen, K.; DuBois, D. L.; Eckert, J.; Fujita, E.; Gibson, D. H.; Goddard, W. A.; Goodman, D. W.; Keller, J.; Kubas, G. J.; Kung, H. H.; Lyons, J. E.; Manzer, L. E.; Marks, T. J.; Morokuma, K.; Nicholas, K. M.; Periana, R.; Que, L.; Rostrup-Nielsen, J.; Sachtler, W. M. H.; Schmidt, L. D.; Sen, A.; Somorjai, G. A.; Stair, P. C.; Stults, B. R.; Tumas, W. *Chem. Rev.* **2001**, *101*, 953–996.

(5) Tsai, J. C.; Nicholas, K. M. *J. Am. Chem. Soc.* **1992**, *114*, 5117–5124.

(6) Leitner, W.; Dinjus, E.; Gassner, F. *J. Organomet. Chem.* **1994**, *475*, 257–266.

(7) Gassner, F.; Dinjus, E.; Gørls, H.; Leitner, W. *Organometallics* **1996**, *15*, 2078–2082.

(8) Yin, C. Q.; Xu, Z. T.; Yang, S. Y.; Ng, S. M.; Wong, K. Y.; Lin, Z. Y.; Lau, C. P. *Organometallics* **2001**, *20*, 1216–1222.

(9) Munshi, P.; Main, A. D.; Linehan, J. C.; Tai, C. C.; Jessop, P. G. *J. Am. Chem. Soc.* **2002**, *124*, 7963–7971.

(10) Tai, C. C.; Pitts, J.; Linehan, J. C.; Main, A. D.; Munshi, P.; Jessop, P. G. *Inorg. Chem.* **2002**, *41*, 1606–1614.

(11) Katho, A.; Opre, Z.; Laurency, G.; Joo, F. *J. Mol. Catal. A: Chem.* **2003**, *204*, 143–148.

(12) Tai, C. C.; Chang, T.; Roller, B.; Jessop, P. G. *Inorg. Chem.* **2003**, *42*, 7340–7341.

(13) Hayashi, H.; Ogo, S.; Fukuzumi, S. *Chem. Commun.* **2004**, 2714–2715.

(14) Ng, S. M.; Yin, C. Q.; Yeung, C. H.; Chan, T. C.; Lau, C. P. *Eur. J. Inorg. Chem.* **2004**, 1788–1793.

(15) Fornika, R.; Gørls, H.; Seemann, B.; Leitner, W. *J. Chem. Soc., Chem. Commun.* **1995**, 1929–1929.

(16) Fornika, R.; Dinjus, E.; Gørls, H.; Leitner, W. *J. Organomet. Chem.* **1996**, *511*, 145–155.

(17) Graf, E.; Leitner, W. *Chem. Ber.* **1996**, *129*, 91–96.

(18) Hutschka, F.; Dedieu, A.; Leitner, W. *Angew. Chem., Int. Ed. Engl.* **1995**, *34*, 1742–1745.

(19) Hutschka, F.; Dedieu, A.; Eichberger, M.; Fornika, R.; Leitner, W. *J. Am. Chem. Soc.* **1997**, *119*, 4432–4443.

(20) Sakaki, S.; Musashi, Y. *Int. J. Quantum Chem.* **1996**, *57*, 481–491.

(21) Musashi, Y.; Sakaki, S. *J. Chem. Soc., Dalton Trans.* **1998**, 577–583.

(22) Musashi, Y.; Sakaki, S. *J. Am. Chem. Soc.* **2000**, *122*, 3867–3877.

(23) Musashi, Y.; Sakaki, S. *J. Am. Chem. Soc.* **2002**, *124*, 7588–7603.

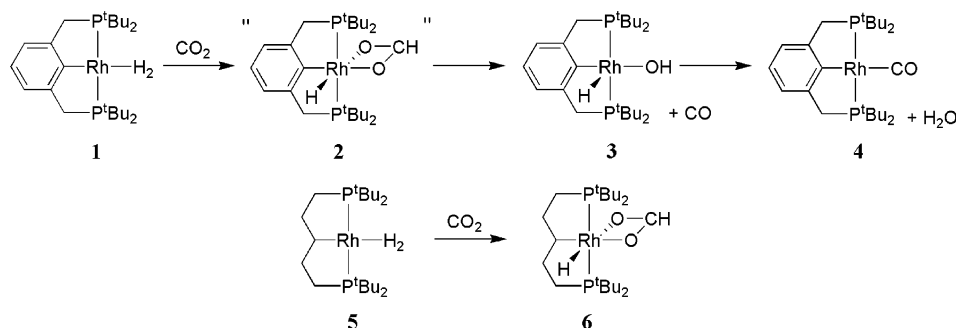
(24) Ohnishi, Y. Y.; Matsunaga, T.; Nakao, Y.; Sato, H.; Sakaki, S. *J. Am. Chem. Soc.* **2005**, *127*, 4021–4032.

(25) Ohnishi, Y. Y.; Nakao, Y.; Sato, H.; Sakaki, S. *Organometallics* **2006**, *25*, 3352–3363.

(26) Kaska, W. C.; Nemeš, S.; Shirazi, A.; Potuznik, S. *Organometallics* **1988**, *7*, 13–15.

(27) Moulton, C. J.; Shaw, B. L. *J. Chem. Soc., Dalton Trans.* **1976**, 1020–1024.

(28) Nemeš, S.; Jensen, C.; Binamirasoriaga, E.; Kaska, W. C. *Organometallics* **1983**, *2*, 1442–1447.

Scheme 1. Reduction of CO₂ by PCP–Rh–H₂ Complexes

further reacted in one week or longer to give a rhodium–carbonyl complex (**4**) and water as final products (Scheme 1). A similar system was studied by Milstein and co-workers in 1996, using a saturated PCP ligand analogue.²⁹ They demonstrated that complex **5** was a nonclassical dihydrogen complex based on the short T_1 (30–60 ms) observed in ¹H NMR. In sharp contrast to Kaska's results, this dihydrogen complex reacted with CO₂ to give a hydridorhodium formate complex (**6**) as the final product without further reactions.

Although these reactions are not catalytic, the different reactivities of these two ligand systems are intriguing. Mechanistic studies on the CO₂ reduction by such complexes would provide a deeper understanding of these processes and could allow the development of new catalyst models for the reduction of CO₂. In this paper, we report computational studies and experimental evidence to determine the binding modes of these PCP–Rh–H₂ complexes and to address the possible reaction pathway for a bound H₂ molecule to reduce CO₂. By comparing the reaction profiles of the aromatic and saturated PCP–Rh models, a probable key step that may be involved in the formation of complex **4** in the aromatic system is also discussed.

Results and Discussion

Coordination Modes of H₂. The relative energies of rotamers of dihydrogen complexes as well as their dihydride isomers were evaluated by DFT calculations using the KMLYP density functional³⁰ to determine the most stable coordination modes of complexes **1** and **5**. In addition to the real *tert*-butyl structures, the hypothetical truncated hydrogen models were also studied.

Complex **5** was chosen to be studied first in order to support Milstein's results. Three isomers were located for this saturated PCP model: the η^2 -dihydrogen complex **5a**, where the H–H bond is perpendicular to the PCP–Rh plane, the η^2 -dihydrogen complex **5b**, where the H–H bond is parallel to the PCP–Rh plane, and the dihydride isomer **5c** (Figure 1). The H(a)–H(b) distances in **5a** and **5b** are 0.830 and 0.821 Å, respectively, and fall into the range of typical H–H bond lengths in nonclassical dihydrogen transition metal complexes.^{31–34} The H(a)–Rh and H(b)–Rh bond distances in **5a** and **5b** are ~0.25 and ~0.1 Å longer than the H(a)–Rh bond and the H(b)–Rh bond in **5c**, respectively. All the structures of the PCP–Rh framework in these three isomers are similar and comparable

to that of the hydridorhodium chloride structure (PCP–Rh(H)–Cl) determined by X-ray crystallography.³⁵ Frequency calculations were used to verify that calculated structures were indeed minima and to determine zero-point energies and entropic contributions to the free energies. Calculated relative free energies show that **5a** is more stable than **5b** and **5c** by 1.1 and 7.0 kcal/mol at 25 °C (298.15 K), consistent with the experimental observations that complex **5** exists as a η^2 -dihydrogen complex.²⁹

For the aromatic complex **1**, three isomers were located as well. In general, they show similar structural patterns to their corresponding complex **5** analogues. Noteworthy is that the P1–Rh–P2 planes are distorted from the phenyl rings in these structures to give dihedral angles for P2–Rh–C3–C4 of 12.5°, 12.9°, and 11.1° for **1a**, **1b**, and **1c**, respectively.²⁸ Moreover, in **1a** the H–H bond is found to be perpendicular to the phenyl plane, and in **1b** the H–H bond is almost parallel to the P1–Rh–P1 plane (Figure 2). In an effort to elucidate the orientation preference of the H–H bond, the molecular orbitals of **1a** and **1b** were analyzed. As shown in Figure 3, both HOMO–7 orbitals in **1a** and **1b** show that the H–H binding angle has no significant effect on the σ interaction of the bonding orbital of H₂ to the Rh center. However, in terms of the $d\pi$ back-donation from Rh to the σ^* orbital of H₂, the H–H binding angles can induce different interactions with other ligands. The HOMO–1 of **1a** involves antibonding between the $d\pi$ orbital of Rh and the π orbital of the phenyl ring, and the HOMO–4 of **1b** consists of interactions with the Rh–P bonds.³⁶ These observations suggest that the back-donation from the transition metal–ligand fragment to σ^* of H₂ plays an important role in determining the orientation of the H–H axis.

A similar trend in relative stabilities was observed. The dihydrogen complex **1a** is more stable than complex **1b** and the dihydride complex **1c** by 0.3 and 9.9 kcal/mol, respectively. These results indicate that complex **1** is also a nonclassical dihydrogen complex. To further confirm this assignment, complex **1** was subjected to the T_1 measurement. The synthesis of **1** was carried out by treating the PCP–Rh–(N₂) analogue under 1–2 atm of H₂ to replace the N₂ ligand with H₂.²⁹ Its ¹H, ¹³C, and ³¹P NMR spectroscopic properties were identical to those reported in the literature for **1** via a different synthetic route.²⁸ The T_1 obtained on a Bruker Avance spectrometer (400 MHz) at –45 °C is 26 ± 1 ms,³⁷ supporting the dihydrogen binding mode.²⁹ Moreover, the H–H bond distance of **1** was estimated to be 0.874–0.891 Å, in good agreement with the calculation results, by measuring the H–D coupling constant

(29) Vignalok, A.; BenDavid, Y.; Milstein, D. *Organometallics* **1996**, *15*, 1839–1844.

(30) Kang, J. K.; Musgrave, C. B. *J. Chem. Phys.* **2001**, *115*, 11040–11051.

(31) Kubas, G. J.; Ryan, R. R.; Swanson, B. I.; Vergamini, P. J.; Wasserman, H. J. *J. Am. Chem. Soc.* **1984**, *106*, 451–452.

(32) Morris, R. H.; Sawyer, J. F.; Shiralian, M.; Zubkowski, J. D. *J. Am. Chem. Soc.* **1985**, *107*, 5581–5582.

(33) Kubas, G. J. *Acc. Chem. Res.* **1988**, *21*, 120–128.

(34) Crabtree, R. H. *Acc. Chem. Res.* **1990**, *23*, 95–101.

(35) Crocker, C.; Errington, R. J.; McDonald, W. S.; Odell, K. J.; Shaw, B. L.; Goodfellow, R. J. *J. Chem. Soc., Chem. Commun.* **1979**, 498–499.

(36) Hay, P. J. *J. Chem. Phys. Lett.* **1984**, *103*, 466–469.

(37) Consistent with the reported value: Xu, W.-W.; Rosini, G. P.; Gupta, M.; Jensen, C. M.; Kaska, W. C.; Krogh-Jespersen, K.; Goldman, A. S. *Chem. Commun.* **1997**, 2273–2274.

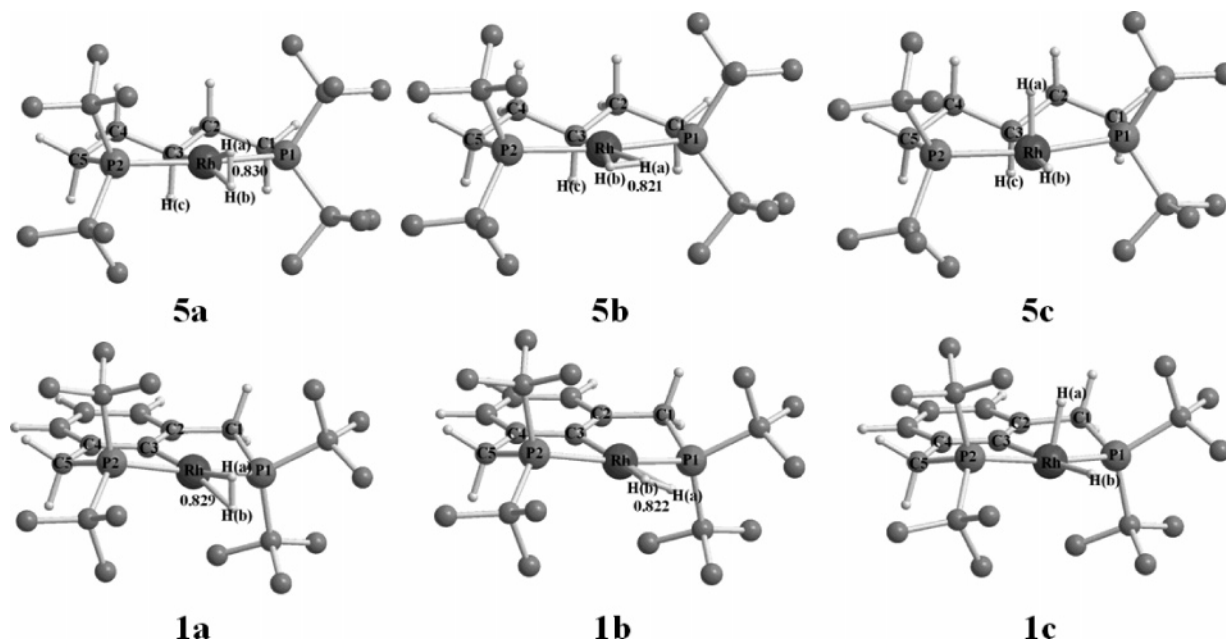


Figure 1. Optimized structures of PCP–Rh–H₂ isomers with hydrogen atoms of the *tert*-butyl groups omitted.

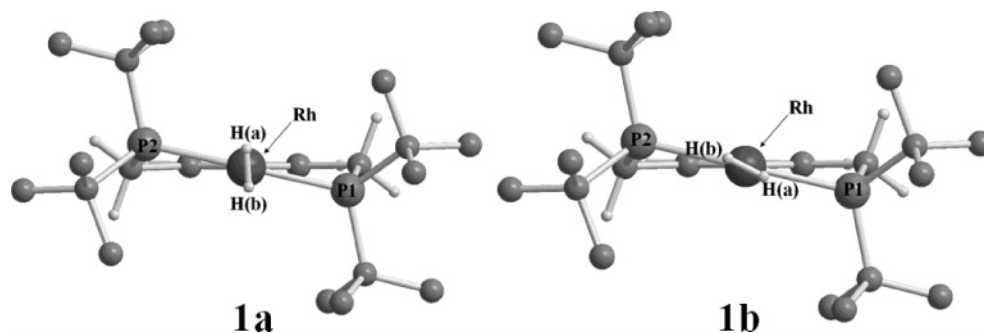


Figure 2. Front views of dihydrogen complexes **1a** and **1b**.

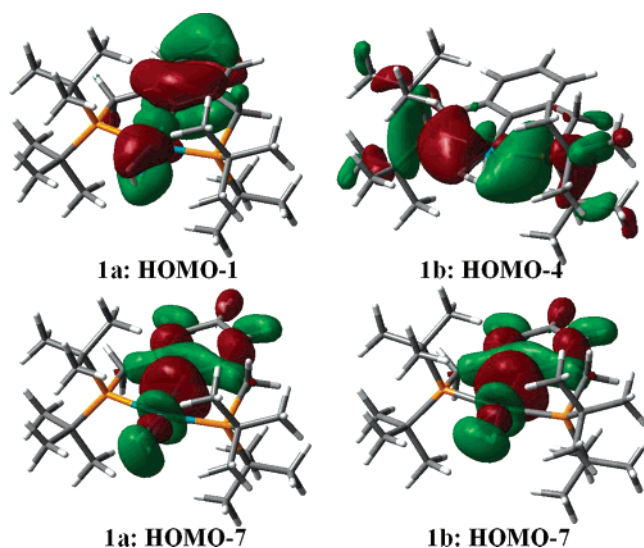


Figure 3. Selected molecular orbitals of dihydrogen complexes **1a** and **1b**.

of the PCP–Rh–(HD) analogue ($J_{\text{HD}} = 32.7$ Hz, at 25 and -45 °C)³⁷ and using the empirical formulas developed by both Morris³⁸ and Heinekey.³⁹

(38) Maltby, P. A.; Schlaf, M.; Steinbeck, M.; Lough, A. J.; Morris, R. H.; Klooster, W. T.; Koetzle, T. F.; Srivastava, R. C. *J. Am. Chem. Soc.* **1996**, *118*, 5396–5407.

(39) Luther, T. A.; Heinekey, D. M. *Inorg. Chem.* **1998**, *37*, 127–132.

Replacement of the *tert*-butyl groups with hydrogen atoms in the truncated models, **7** (H model of **1**) and **8** (H model of **5**), resulted in the complete destabilization of the type **b** dihydrogen rotamers and the type **c** dihydride isomers. All attempts at optimizing these structures led to the type **a** dihydrogen complexes. This could be rationalized by both electronic and steric effects that the *tert*-butyl groups help stabilize the type **b** dihydrogen complexes by increasing the barriers of the Rh–(H₂) bond rotation, and the dihydride complexes by introducing more electron density to the metal center. Nevertheless, the truncated hydrogen models successfully predicted the most stable structures.

Mechanism of CO₂ Reduction. Several important theoretical studies on the Rh-catalyzed hydrogenation of CO₂ to formic acid (HCOOH) have been reported.^{19,21,23} The proposed mechanism involves hydride transfer from a Rh–H bond to a η^1 -O-coordinated CO₂ to form a Rh–formate intermediate, which can then either undergo oxidative addition of an H₂ molecule to the metal center to form a dihydride intermediate followed by the reductive elimination of HCOOH or undergo σ -bond metathesis with H₂ to release HCOOH and regenerate the catalytically active Rh–H complex. As discussed above, even though complexes **1** and **5** are nonclassical dihydrogen complexes, experimental results have established that they can both reduce CO₂ to afford reduction products. Because the dihydrogen complexes were identified as the most stable species, the way the bound H₂ reduces CO₂ is intriguing. To investigate this question, only complexes **7** and **8**, the truncated hydrogen

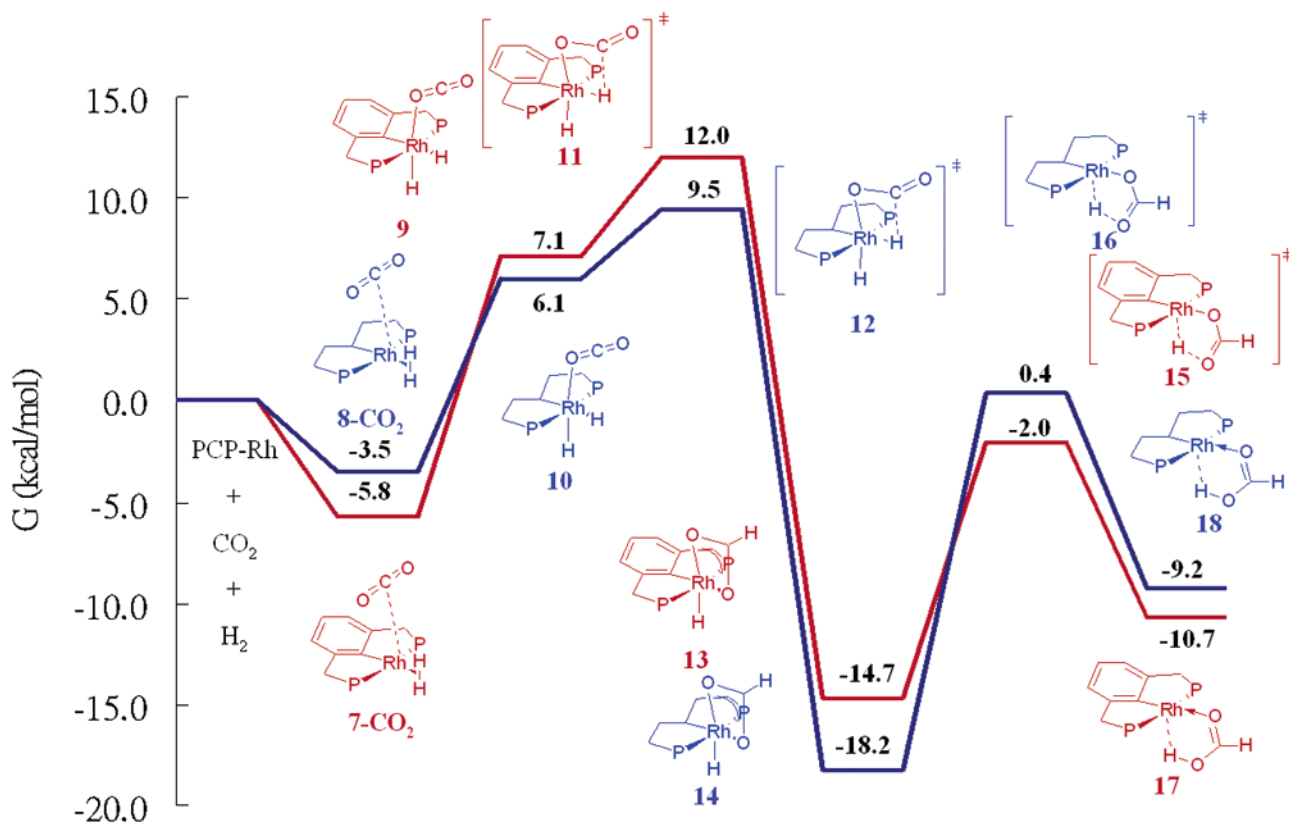


Figure 4. Free-energy changes for the CO₂ reduction processes at 298.15 K. For clarity, the H atoms on the phosphorus atoms have been omitted.

models of **1** and **5**, were employed in the mechanistic study to examine the possible pathways in the interest of computational efficiency. Truncated hydrogen models have been previously applied successfully in other similar pincer systems.^{40–43}

We found that η^2 -H₂ binding followed by CO₂ coordination to a naked PCP-Rh center to give the dihydrogen complex with a weakly bound η^1 -CO₂ complex (Figure 4) is thermodynamically favored. This type of η^1 interaction can be viewed as the donation of the HOMO of the Rh-H₂ complex, a d_z² orbital, to the π^* orbital of the CO₂ molecule. However, the CO₂ coordination is expected to be weak because the Rh-CO₂ distances are 3.411 and 3.274 Å for **7**-CO₂ and **8**-CO₂, respectively. No intermediates or transition states could be derived to connect these two dihydrogen-Rh- η^1 -CO₂ complexes to the CO₂ reduction processes.

We then examined the possible routes for the reduction to proceed through the dihydride structures. Similar to the observed relative energies of the dihydrogen and the dihydride isomers of complexes **1** and **5**, the dihydrido-Rh-CO₂ complexes **9** and **10** are 12.9 and 9.6 kcal/mol, respectively, higher in energy than **7**-CO₂ and **8**-CO₂. We predict that CO₂ binds to Rh in an η^1 -OCO “end-on” fashion in both complexes. Selected bonding parameters and the corresponding atom numberings are summarized in Table 1. Species **9** and **10** both have long Rh-O1 and C2-H(b) distances, but we note that the C2-H(b) distances are 0.3–0.7 Å shorter than those reported in other DFT studies for cationic Rh species.^{21,23} These geometrical features might

suggest that the hydrido-CO₂ interaction is stronger for the neutral PCP-Rh complex bearing a hydride *trans* to the C ligand (phenyl or alkyl).

These dihydride structures can then undergo the hydride transfer from the Rh center to the C center of CO₂ with low-energy barriers. Most of the structural variables of the transition states **11** and **12** do not vary significantly from those of the starting intermediates, except that the C2-H(b) distances become 0.8–0.9 Å shorter and the O1-C2-O2 angles change from linear to $\sim 155^\circ$. The overall energy barriers for the reduction of CO₂ by the PCP-Rh η^1 -H₂ complexes are calculated to be 17.8 kcal/mol for **7** and 13.0 kcal/mol for **8**, consistent with the fact that the reactions of CO₂ with **1** and **5** occur instantly at room temperature.^{26,29} After the hydride insertion event, the kinetic products formed are hydridorhodium η^1 -formate complexes, which should transform into the most stable η^2 -formate coordination compounds, as the d⁶ rhodium center prefers the d²sp³ octahedral structure. The transition state energy of such transformations has been previously estimated to be 2–5 kcal/mol above the η^1 -formate complex by Musashi and Sakaki.²¹ Thus, these calculations were not performed in this study. However, as expected, complexes **13** and **14** were predicted to be the most thermodynamically stable products for the CO₂ reduction reactions. They both have similar C2-O1 and C2-O2 bond lengths and the C2 centers are now sp² hybridized.

Complex **6** has been shown as the final product of the reaction of complex **5** and CO₂.²⁹ In order to verify that the rhodium formate complex **2** was an intermediate formed in the reaction of complex **1** and CO₂, this reaction was monitored by NMR. It was found that complex **2** was formed immediately together with a small amount of an intermediate and the PCP-Rh-CO complex **4**. The lifetime of **2** was long enough under such

(40) Sundermann, A.; Uzan, O.; Milstein, D.; Martin, J. M. L. *J. Am. Chem. Soc.* **2000**, *122*, 7095–7104.

(41) van der Boom, M. E.; Iron, M. A.; Atasoylu, O.; Shimon, L. J. W.; Rozenberg, H.; Ben-David, Y.; Konstantinovski, L.; Martin, J. M. L.; Milstein, D. *Inorg. Chim. Acta* **2004**, *357*, 1854–1864.

(42) Niu, S. Q.; Hall, M. B. *J. Am. Chem. Soc.* **1999**, *121*, 3992–3999.

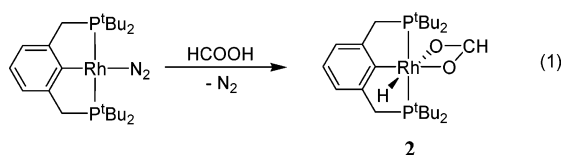
(43) Li, S. H.; Hall, M. B. *Organometallics* **2001**, *20*, 2153–2160.

Table 1. Selected Geometrical Parameters for Complexes 9–18^a

	9	10	11	12	13	14	15	16	15'	16'	17	18	15	16	15'	16'	17	18	17	18				
Rh-C1	2.059	2.148	2.063	2.117	2.006	2.061	2.025	2.076	2.018	2.054	2.017	2.067	2.025	2.076	2.018	2.054	2.017	2.067	2.017	2.067				
Rh-P1	2.268	2.261	2.275	2.269	2.281	2.281	2.282	2.287	2.281	2.287	2.273	2.273	2.282	2.287	2.281	2.287	2.273	2.273	2.273	2.273				
Rh-O1	2.424	2.399	2.315	2.308	2.257	2.232	-	-	-	-	-	-	-	-	-	-	-	-	-	-				
Rh-O2	-	-	-	-	2.215	2.272	2.146	2.184	2.168	2.208	2.220	2.249	2.146	2.184	2.168	2.208	2.220	2.249	2.220	2.249				
Rh-H(a)	1.510	1.514	1.520	1.523	1.537	1.543	1.575	1.605	1.569	1.569	2.181	2.147	1.575	1.605	1.569	1.569	2.181	2.147	2.181	2.147				
Rh-H(b)	1.641	1.654	1.692	1.698	-	-	-	-	-	-	-	-	-	-	-	-	-	-	-	-				
C2-H(b)	2.672	2.611	1.743	1.811	1.093	1.094	1.092	1.092	1.100	1.103	1.085	1.086	1.092	1.092	1.100	1.103	1.085	1.086	1.085	1.086				
C2-O1	1.157	1.159	1.189	1.186	1.243	1.247	1.240	1.246	1.193	1.194	1.292	1.292	1.240	1.246	1.193	1.194	1.292	1.292	1.292	1.292				
C2-O2	1.143	1.143	1.161	1.159	1.243	1.239	1.243	1.238	1.295	1.292	1.204	1.204	1.243	1.238	1.295	1.292	1.204	1.204	1.204	1.204				
O1-H(a)	-	-	-	-	-	-	1.535	1.457	-	-	0.998	1.004	1.535	1.457	-	-	0.998	1.004	0.998	1.004				
O2-H(a)	-	-	-	-	-	-	-	-	1.435	1.424	-	-	-	-	1.435	1.424	-	-	-	-				
O1-C1-O2	175.9	174.8	153.4	155.1	122.2	122.6	125.4	125.1	125.1	125.6	124.1	124.0	125.4	125.1	125.1	125.6	124.1	124.0	124.1	124.0				
P1-Rh-P2	159.8	161.8	161.0	162.8	163.2	167.5	161.1	156.2	162.2	162.7	161.5	162.5	161.1	156.2	162.2	162.7	161.5	162.5	161.5	162.5				

^a Reported in deg and Å.

conditions to allow a ¹H, ¹³C, and ³¹P NMR analysis. The ¹³C-¹H NMR chemical shift of the formate carbon atom is δ 172.4 ppm, consistent with Kaska's observation when using ¹³CO₂.²⁶ The ³¹P-¹H NMR chemical shift at δ 78.0 ppm, with a J_{RhP} coupling constant of 118.4 Hz, indicates a Rh(III) formal oxidation state. Unfortunately, due to its instability, complex **2** could not be isolated and purified. Thus, to further confirm that the intermediate we observed was indeed the rhodium formate complex, complex **2** was also prepared by treating PCP-Rh-(N₂) with an excess amount of HCOOH (eq 1). The resulting ¹H, ¹³C, and ³¹P NMR spectroscopic properties were identical to those observed from the reaction of complex **1** and CO₂. Furthermore, when HCOOD was used, the proton NMR signal for Rh-H at δ -22.51 ppm was not detected, and when DCOOH was used, the signal of the formyl hydrogen (Rh-O₂CH) at δ 8.64 ppm was not observed. Using H¹³COOH led to a doublet signal for Rh-O₂CH at δ 8.64 ppm with a J_{CH} coupling constant of 194 Hz, consistent with the literature value measured by ¹³C NMR.²⁶



Reductive Elimination of Formic Acid. Kaska and co-workers have demonstrated that the short-lived complex **2** further decomposed to give the Rh-CO complex **4** and water as the final products under CO₂.²⁶ The two major reactions of hydrido transition metal formate complexes reported in the literature are decarboxylation via β -hydride elimination to lose CO₂,⁴⁴ a reverse reaction of the hydride transfer to CO₂, and the reductive elimination of formic acid.^{2,6} Since the decarboxylation reaction will result in the regeneration of complex **1** and CO₂, it is inferred that the formation of complex **4** can only occur after the reductive elimination of a formic acid molecule from **2** followed by the decarbonylation of the formyl

functional group of the formic acid by the reduced Rh(I) center, given the fact that Rh(I) compounds are excellent decarbonylation reagents for aldehydes and formate esters.⁴⁵⁻⁴⁹

The reductive elimination reactions were examined by DFT for the hydrogen analogues **13** and **14** (Table 1 and Figure 4). Only the five-centered transition states, **15** and **16**, and the three-centered ones, **15'** and **16'**, were studied because the dihydrogen-induced σ -bond metathesis for the elimination of a formic acid molecule was not possible in these reaction conditions.^{26,29} Consistent with Musashi and Sakaki's observations,²³ transition states **15'** and **16'** are of much higher energies than **15** and **16** by 24.3 and 19.9 kcal/mol, respectively, thus indicating that the five-centered transition states are also more favored for these pincer complexes. The reductive elimination reactions through the five-centered transition states led to the most stable Rh(I)- κ^2 -formic acid adducts, **17** and **18**. Despite the fact that the reaction patterns of the aromatic and saturated PCP complexes are similar, it should be noted that the transition state barrier for reductive elimination of **14** is 5.9 kcal/mol higher than that of **13**, and the energy difference between the hydridorhodium η^2 -formate complex and the Rh(I)- κ^2 -formic acid product for **14** and **18** is also 5.0 kcal/mol larger than those for **13** and **17**. We rationalize this by noting that the saturated PCP ligand makes the rhodium center more electron rich and, thus, disfavors the reductive elimination reaction.⁵⁰ These results suggest that if the elimination reaction of formic acid is an essential step for a subsequent decarbonylation reaction to occur, complex **2** will be much more reactive than complex **6**.

Conclusion

In summary, we have employed the KMLYP DFT functional to perform a mechanistic study of CO₂ reduction reactions

(45) Ohno, K.; Tsuji, J. *J. Am. Soc. Chem.* **1968**, *90*, 99 - 107.

(46) Walborsky, H. M.; Allen, L. E. *J. Am. Chem. Soc.* **1971**, *93*, 5465-5468.

(47) Zahalka, H. A.; Alper, H. *Tetrahedron Lett.* **1987**, *28*, 2215-2216.

(48) Oconnor, J. M.; Ma, J. *J. Org. Chem.* **1992**, *57*, 5075-5077.

(49) Beck, C. M.; Rathmill, S. E.; Park, Y. J.; Chen, J. Y.; Crabtree, R. H.; Liable-Sands, L. M.; Rheingold, A. L. *Organometallics* **1999**, *18*, 5311-5317.

(50) Zhao, J.; Goldman, A. S.; Hartwig, J. F. *Science* **2005**, *307*, 1080-1082.

(44) Kim, Y.; Rende, D. E.; Gallucci, J. C.; Wojcicki, A. *J. Organomet. Chem.* **2003**, *682*, 85-101.

mediated by pincer PCP–Rh dihydrogen complexes. Consistent with the experimental observations, complexes **1** and **5** were both identified as *nonclassical dihydrogen complexes*. Although the η^2 -dihydrogen structures are thermodynamically favored over dihydride isomers, in order to reduce the bound CO₂ molecule, *hydride transfer from the Rh center to carbon must proceed through the dihydride intermediate*. These results further suggest that CO₂ reduction by hydrogen does not necessarily require a metal hydride precursor as long as a hydride intermediate is thermodynamically accessible. The formation of hydridorhodium formate **2** was confirmed experimentally by NMR in the reaction of the η^2 -dihydrogen complex **1** with CO₂. Complex **2** was also prepared independently and characterized by NMR techniques. Investigations on the probable HCOOH reductive elimination reactions from the truncated hydrido-rhodium formate models **13** and **14** revealed that the energy barrier and the corresponding free energy of reaction for the saturated PCP model **14** are 5.9 and 5.0 kcal/mol higher, respectively, than those of the aromatic analogue **13**. This observation suggests that the more electron-donating saturated PCP complex disfavors the reductive elimination. Computational and experimental investigations of the mechanism of the subsequent decarbonylation from complex **2** are currently ongoing in our laboratories.

Computational and Experimental Details

Computational Details. DFT calculations on the PCP–rhodium complexes were performed using the Gaussian 03 program (revision C.02).⁵¹ The KMLYP hybrid DFT method was employed.³⁰ This method combines the HF and Slater exchange functionals⁵² for the exchange energy and the VWN⁵³ and LYP⁵⁴ correlation functionals for the correlation energy. The mixing parameters were obtained in an attempt to reduce self-interaction errors generally present in most DFT methods by reproducing the ground state energy of atomic hydrogen, while simultaneously describing electron–electron interactions by reproducing the electron affinity of atomic oxygen. KMLYP has been shown to correctly determine a wide variety of molecular properties for significantly different systems.^{55–58} Geometry optimizations were performed using the default convergence criteria without any geometric constraints. The LANL2DZ ECP

basis set^{59–61} was used for the rhodium atom, while the all-electron 6-31G+(d) Pople basis set was employed for all other atoms.^{62–64} Frequency calculations were used to characterize the stationary points as minima or transition state structures, to determine zero-point energies (ZPEs), and for free-energy calculations. Gibbs free energies were calculated at 25 °C (298.15 K).

General Procedures. All manipulations were carried out under an atmosphere of nitrogen using Schlenk techniques or in a MBraun drybox. ¹H, ¹³C{¹H}, and ³¹P{¹H} NMR spectra were recorded on a Bruker Avance spectrometer (400 MHz for ¹H, 125 MHz for ¹³C, and 161.98 MHz for ³¹P). ¹H NMR chemical shifts were referenced to the residual proton peak of *d*₆-benzene (C₆D₆) at δ 7.15, ¹³C NMR chemical shifts were referenced to C₆D₆ at δ 128.0, and ³¹P NMR chemical shifts were referenced to an external 85% H₃PO₄ sample at δ 0.0. C₆D₆ was distilled from purple sodium/benzophenone solution and stored under N₂ prior to use. Complexes **1** and **5** were synthesized from their dinitrogen analogues upon treatment of dihydrogen atmosphere according to the literature procedures.²⁹ Research grades of N₂, H₂, and CO₂ were used without further purification. HCOOD (98% D, <5% D₂O), DCOOH (98% D, <5% H₂O), and H¹³COOH (99% ¹³C, <5% H₂O) were purchased from Cambridge Isotope Laboratories, Inc. and degassed by three freeze–pump–thaw cycles prior to use.

{2,6-Bis[(di-*tert*-butylphosphino)methyl]phenyl}hydridorhodium Formate, 2. A solution of PCP–Rh–(H₂) complex **1**, synthesized by treating 1.0 mg of {2,6-bis[(di-*tert*-butylphosphino)methyl]phenyl}rhodium dinitrogen complex in 0.7 mL of *d*₆-benzene under 1 atm of H₂, was fully degassed and then saturated under 2 atm of CO₂ at room temperature. Complex **2** was formed immediately together with a small amount of an intermediate and PCPRh–CO **4** (less than 5%). ¹H NMR (C₆D₆): δ –22.51 (dt, 1H, *J*_{RhH} = 31.7 Hz, *J*_{PH} = 12.2 Hz), 1.21 (t, 18H, *J*_{PH} = 6.7 Hz), 1.30 (t, 18H, *J*_{PH} = 6.4 Hz), 2.85 (dt, 2H, *J*_{RhH} = 17.1 Hz, *J*_{PH} = 3.6 Hz), 3.13 (dt, 2H, *J*_{RhH} = 17.1 Hz, *J*_{PH} = 3.6 Hz), 6.85–7.00 (m, 3H), 8.64 (s, 1H). ¹³C{¹H} NMR (C₆D₆): δ 29.7 (t, *J*_{PC} = 2.7 Hz), 30.0 (t, *J*_{PC} = 3.1 Hz), 33.3 (dt, *J*_{RhC} = 3.0 Hz, *J*_{PC} = 10.7 Hz), 35.1 (dt, *J*_{RhC} = 1.5 Hz, *J*_{PC} = 8.5 Hz), 36.5 (t, *J*_{PC} = 6.8 Hz), 122.1 (t, *J*_{PC} = 8.5 Hz), 122.8 (s), 149.5 (t, *J*_{PC} = 10.0 Hz), 155.5 (d, *J*_{RhC} = 42.9 Hz), 172.4 (s). ³¹P{¹H} NMR (C₆D₆): δ 78.0 (d, *J*_{RhP} = 118.4 Hz). Treatment of the PCP–Rh–(N₂) *d*₆-benzene solution with 25 equiv of formic acid afforded a complex with the NMR properties identical with those of complex **2**.

Acknowledgment. This work is supported by Brookhaven National Laboratory under contact DE-AC02-98CH10886 with the U.S. Department of Energy. We thank Drs. Morris Bullock and David Grills at BNL for useful discussions. K.-W.H. acknowledges a Gertrude and Maurice Goldhaber Distinguished Fellowship. This paper is dedicated to Professor Tien-Yau Luh.

Supporting Information Available: Further details of the DFT computational results. This material is available free of charge via the Internet at <http://pubs.acs.org>.

OM060797O

(51) Frisch, M. J.; Trucks, G. W.; Schlegel, H. B.; Scuseria, G. E.; Robb, M. A.; Cheeseman, J. R.; Zakrzewski, V. G.; Montgomery, J. A., Jr.; Stratmann, R. E.; Burant, J. C.; Dapprich, S.; Millam, J. M.; Daniels, A. D.; Kudin, K. N.; Strain, M. C.; Farkas, O.; Tomasi, J.; Barone, V.; Cossi, M.; Cammi, R.; Mennucci, B.; Pomelli, C.; Adamo, C.; Clifford, S.; Ochterski, J.; Petersson, G. A.; Ayala, P. Y.; Cui, Q.; Morokuma, K.; Rega, N.; Salvador, P.; Dannenberg, J. J.; Malick, D. K.; Rabuck, A. D.; Raghavachari, K.; Foresman, J. B.; Cioslowski, J.; Ortiz, J. V.; Baboul, A. G.; Stefanov, B. B.; Liu, G.; Liashenko, A.; Piskorz, P.; Komaromi, I.; Gomperts, R.; Martin, R. L.; Fox, D. J.; Keith, T.; Al-Laham, M. A.; Peng, C. Y.; Nanayakkara, A.; Challacombe, M.; Gill, P. M. W.; Johnson, B.; Chen, W.; Wong, M. W.; Andres, J. L.; Gonzalez, C.; Head-Gordon, M.; Replogle, E. S.; Pople, J. A. *Gaussian 03, Revision C.02*; Gaussian Inc.: Wallingford, CT, 2004.

(52) Slater, J. C. *Quantum Theory of Molecular and Solids: The Self-Consistent Field for Molecular and Solids*; McGraw-Hill: New York, 1974; Vol. 4.

(53) Vosko, S. H.; Wilk, L.; Nusair, M. *Can. J. Phys.* **1980**, *58*, 1200–1211.

(54) Lee, C. T.; Yang, W. T.; Parr, R. G. *Phys. Rev. B* **1988**, *37*, 785–789.

(55) Senosiain, J. P.; Han, J. H.; Musgrave, C. B.; Golden, D. M. *Faraday Discuss.* **2001**, *119*, 173–189.

(56) Kang, J. K.; Musgrave, C. B. *J. Chem. Phys.* **2002**, *116*, 9907–9913.

(57) Song, S. H.; Golden, D. M.; Hanson, R. K.; Bowman, C. T.; Senosiain, J. P.; Musgrave, C. B.; Friedrichs, G. *Int. J. Chem. Kinet.* **2003**, *35*, 304–309.

(58) Pomerantz, A. E.; Han, J. H.; Musgrave, C. B. *J. Phys. Chem. A* **2004**, *108*, 4030–4035.

(59) Hay, P. J.; Wadt, W. R. *J. Chem. Phys.* **1985**, *82*, 299–310.

(60) Hay, P. J.; Wadt, W. R. *J. Chem. Phys.* **1985**, *82*, 270–283.

(61) Wadt, W. R.; Hay, P. J. *J. Chem. Phys.* **1985**, *82*, 284–298.

(62) Ditchfie, R.; Hehre, W. J.; Pople, J. A. *J. Chem. Phys.* **1971**, *54*, 724–728.

(63) Hehre, W. J.; Ditchfie, R.; Pople, J. A. *J. Chem. Phys.* **1972**, *56*, 2257–2261.

(64) Harihara, P. C.; Pople, J. A. *Theor. Chim. Acta* **1973**, *28*, 213–222.